Eur. Phys. J. D **25**, 173–180 (2003)
DOI: 10.1140/epjd/e2003-00095-7

THE EUROPEAN PHYSICAL JOURNAL D

Two-time synchronism and induced synchronization in a Kerr coupler

P. Szlachetka[a], M. Misiak[b], and K. Grygiel[c]

Nonlinear Optics Division[d], Institute of Physics, A. Mickiewicz University, ul. Umultowska 85, 61-614 Poznań, Poland

Received 9 August 2002 / Received in final form 20 February 2003
Published online 29 April 2003

Abstract. A pair $(\mathbf{A}, \mathbf{B})$ of interacting Kerr oscillators treated as a *master* coupler sending chaotic or hyperchaotic signals to its *slave* copy $(\mathbf{a}, \mathbf{b})$ is considered. We synchronize $\mathbf{a}$ with $\mathbf{A}$ and $\mathbf{b}$ with $\mathbf{B}$ through two communication channels $\mathbf{A} \Rightarrow \mathbf{a}$ and $\mathbf{B} \Rightarrow \mathbf{b}$. The effect of synchronization is non-simultaneous, the pairs $(\mathbf{a}, \mathbf{A})$ and $(\mathbf{b}, \mathbf{B})$ have different times of synchronization. It is possible to synchronize an individual pair, for example, $(\mathbf{b}, \mathbf{B})$ when its communication channel $\mathbf{B} \Rightarrow \mathbf{b}$ is turned off, provided that the second channel for the pair $(\mathbf{a}, \mathbf{A})$ is turned on. The resulted synchronization is termed induced. The efficiencies of the presented synchronization precesses are studied.

PACS. 05.45.Xt Synchronizations; coupled oscillators – 05.45.Pq Numerical simulations of chaotic systems – 42.65.Sf Dynamics of nonlinear optical systems; optical instabilities, optical chaos and complexity, and optical spatio-temporal dynamics

1 Introduction

Recently, there has been a great deal of interest in the study of coupled oscillators and their role in explaining the basic features of man-made and natural systems. Such systems can exhibit on-off intermittency [1], two-state on-off intermittency [2] or beats with chaotic envelopes [3, 4]. In particular, much attention has been paid to synchronization of chaotic systems (for an up-to-date review, see Ref. [5]). Different types of synchronization have been considered, for example, complete synchronization [6–9], partial synchronization [10,11], generalized synchronization [12–15] or phase synchronization [16,17]. Especially, the problem of synchronization of coupled chaotic oscillators has been intensively studied mainly in view of a potential application to secure communication [18–23]. The idea of synchronization has also been implemented in higher dimensional systems exhibiting hyperchaotic behavior [24–26]. There are also examples of synchronization in optical systems. Many potential applications are expected in coupled laser systems [27–29], especially to secure optical communication [30,31]. Quite recently, the synchronization effects between two Kerr oscillators [32] and between two systems generating second-harmonic of light were found [33].

Frequently, in many optical applications, a multidimensional system can be considered as a coupler of the same or different interacting nonlinear oscillators (for a review, see Ref. [34]). Then, in a synchronization process, individual *master* oscillators are linked to *slave* oscillators through synchronization channels. The general synchronization set-up to be considered is presented in Figure 1. The master system consists of two coupled oscillators $(\mathbf{A}, \mathbf{B})$ interacting with each other (the symbol α denotes a parameter of interaction between $\mathbf{A}$ and $\mathbf{B}$). If $\alpha = 0$, the master coupler consists of two independent oscillators. The slave coupler $(\mathbf{a}, \mathbf{b})$ is a copy of the master one. The signals X_A and X_B from $(\mathbf{A}, \mathbf{B})$ are transmitted to $(\mathbf{a}, \mathbf{b})$ by differential feedback terms $S_1(X_A - X_a)$ and $S_2(X_B - X_b)$. The control parameters are denoted by S_1 and S_2, respectively. The master and slave couplers starting from different initial conditions generate different chaotic signals which are to be synchronized.

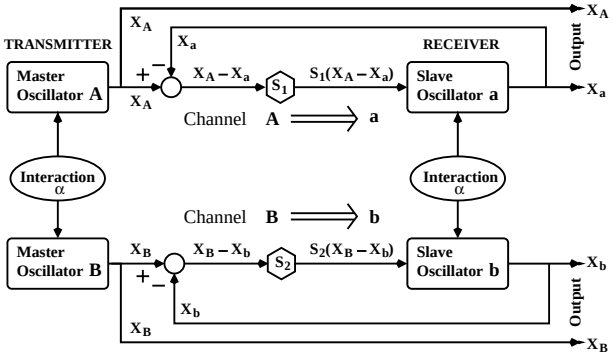

Fig. 1. Schematic diagram of two-channel synchronization. Signals from two interacting master oscillators $\mathbf{A}$ and $\mathbf{B}$ are sent to a system containing two corresponding slave oscillators $\mathbf{a}$ and $\mathbf{b}$. The signals are controlled by the parameters S_1 and S_2. Synchronization is achieved if the output signals satisfy the relations $X_a = X_A$ and $X_b = X_B$.

[a] e-mail: przems@main.amu.edu.pl
[b] e-mail: misiak@zon10.physd.amu.edu.pl
[c] e-mail: grygielk@main.amu.edu.pl
[d] URL: http://zon8.physd.amu.edu.pl

In this paper, we study a possibility of synchronization of two optical Kerr couplers $(\mathbf{A},\mathbf{B})$ and $(\mathbf{a},\mathbf{b})$ on the basis of the schematic diagram presented in Figure 1. The first question is whether and when the individual drive-driven oscillators $(\mathbf{a},\mathbf{A})$ and $(\mathbf{b},\mathbf{B})$ have different times of synchronization. The next question is whether both couplers can be synchronized if one of the synchronization channels has been turned off. And finally, whether the partial synchronization of the couplers is possible, *i.e.* whether only one of the pairs $(\mathbf{a},\mathbf{A})$ or $(\mathbf{b},\mathbf{B})$ can be synchronized, while the other cannot.

2 The model

Let us consider an optical system $(\mathbf{A},\mathbf{B})$ which consists of two Kerr oscillators. They interact with each other and are pumped by time external fields. The Hamiltonian of the system has the form:

$$H = H_{\rm Kerr} + H_{\rm int} + H_{\rm ext}, \tag{1}$$

$$H_{\rm Kerr} = \omega_0 X_A^* X_A + \omega_0 X_B^* X_B + \epsilon X_A^{*2} X_A^2 + \epsilon X_B^{*2} X_B^2, \tag{2}$$

$$H_{\rm int} = -\frac{\alpha}{2}\left(X_A^* X_B + X_A X_B^*\right) - \frac{\alpha}{2}\left(X_A^* X_B^* + X_A X_B\right), \tag{3}$$

$$H_{\rm ext} = -(\sqrt{2})^{-1} F\left[(X_A^* + X_A)\cos\Omega_1 t + (X_B^* + X_B)\cos\Omega_2 t\right], \tag{4}$$

where the terms $\omega_0 X_A^* X_A$ and $\omega_0 X_B^* X_B$ describe simple harmonic oscillators, both with the natural frequencies ω_0. The dynamical variables X_A and X_B are the complex amplitudes of modes $\mathbf{A}$ and $\mathbf{B}$, respectively. The parameter of Kerr nonlinearity is denoted by ϵ. The interaction between the Kerr oscillators is governed by the Hamiltonian (3), where α is an interaction parameter. If the rotational terms $(X_A^* X_B^* + X_A X_B)$ are neglected, the interaction Hamiltonian (3) is in the so-called rotating wave approximation (RWA). The Kerr oscillators are pumped by the external time-dependent fields with the amplitude F and frequencies Ω_1 and Ω_2, respectively. The Hamiltonians (1–4) have a very simple form in the momentum-position representation (p,q). Putting $\omega_0 = 1$ and taking into account the canonical transformation $X_{A,B} = (\sqrt{2})^{-1}(q_{A,B} + {\rm i}p_{A,B})$ and $X_{A,B}^* = (\sqrt{2})^{-1}(q_{A,B} - {\rm i}p_{A,B})$ we get

$$H = H_{\rm Kerr} + H_{\rm int} + H_{\rm ext}, \tag{5}$$

$$H_{\rm Kerr} = \left(p_A^2/2 + q_A^2/2\right) + \epsilon\left(p_A^2/2 + q_A^2/2\right)^2 + \left(p_B^2/2 + q_B^2/2\right) + \epsilon\left(p_B^2/2 + q_B^2/2\right)^2, \tag{6}$$

$$H_{\rm int} = -\alpha q_A q_B, \tag{7}$$

$$H_{\rm ext} = -F\left(q_A\cos\Omega_1 t + q_B\cos\Omega_2 t\right). \tag{8}$$

If the interaction Hamiltonian (3) is in the rotating wave approximation then additionally, a momentum-momentum interaction appears in (7), consequently we have $H_{\rm int} = -\alpha(q_A q_B + p_A p_B)$. If $\epsilon = 0$, the Hamiltonian (5–8) describes a standard text-book model of two coupled linear subsystems.

The Hamiltonian (1–4) with $\omega_0 = 1$ leads to the following equations of motion [32]:

$$\frac{{\rm d}X_A}{{\rm d}t} = -{\rm i}X_A - \gamma_A X_A - 2{\rm i}\epsilon X_A^* X_A^2 + {\rm i}\frac{\alpha}{2}(X_B + X_B^*) + {\rm i}(\sqrt{2})^{-1} F\cos\Omega_1 t, \tag{9}$$

$$\frac{{\rm d}X_B}{{\rm d}t} = -{\rm i}X_B - \gamma_B X_B - 2{\rm i}\epsilon X_B^* X_B^2 + {\rm i}\frac{\alpha}{2}(X_A + X_A^*) + {\rm i}(\sqrt{2})^{-1} F\cos\Omega_2 t, \tag{10}$$

where the damping terms $\gamma_{A,B}X_{A,B}$ have been added phenomenologically. The coefficients $\gamma_{A,B}$ are damping constants. The linear terms ${\rm i}\frac{\alpha}{2}(X_B + X_B^*)$ and ${\rm i}\frac{\alpha}{2}(X_A + X_A^*)$ in the above equations of motion are responsible for the interactions between individual Kerr oscillators. In the RWA-case the variables X_B^* and X_A^* do not appear in the equations of motion. The slave coupler is a replica of the master coupler (9, 10), where $\mathbf{A}\to\mathbf{a}$ and $\mathbf{B}\to\mathbf{b}$. According to the continuous feedback method [6,36], our master coupler $(\mathbf{A},\mathbf{B})$ is coupled to the slave coupler $(\mathbf{a},\mathbf{b})$ in the following way

$$\frac{{\rm d}X_a}{{\rm d}t} = -{\rm i}X_a - \gamma_a X_a - 2{\rm i}\epsilon X_a^* X_a^2 + {\rm i}\frac{\alpha}{2}(X_b + X_b^*) + {\rm i}(\sqrt{2})^{-1} F\cos\Omega_1 t + S_1(X_A - X_a), \tag{11}$$

$$\frac{{\rm d}X_b}{{\rm d}t} = -{\rm i}X_b - \gamma_b X_b - 2{\rm i}\epsilon X_b^* X_b^2 + {\rm i}\frac{\alpha}{2}(X_a + X_a^*) + {\rm i}(\sqrt{2})^{-1} F\cos\Omega_2 t + S_2(X_B - X_b). \tag{12}$$

For numerical studies it is convenient to rewrite equations (9–12) in real variables, we get the following eight equations of motion:

$$\frac{{\rm d}q_A}{{\rm d}t} = p_A[1 + \epsilon(p_A^2 + q_A^2)] - \gamma_A q_A, \tag{13}$$

$$\frac{{\rm d}p_A}{{\rm d}t} = -q_A[1 + \epsilon(p_A^2 + q_A^2)] - \gamma_A p_A + \alpha q_B + F\cos\Omega_1 t, \tag{14}$$

$$\frac{{\rm d}q_B}{{\rm d}t} = p_B[1 + \epsilon(p_B^2 + q_B^2)] - \gamma_B q_B, \tag{15}$$

$$\frac{{\rm d}p_B}{{\rm d}t} = -q_B[1 + \epsilon(p_B^2 + q_B^2)] - \gamma_B p_B + \alpha q_A + F\cos\Omega_2 t, \tag{16}$$

$$\frac{{\rm d}q_a}{{\rm d}t} = p_a[1 + \epsilon(p_a^2 + q_a^2)] - \gamma_a q_a + S_1(q_A - q_a), \tag{17}$$

$$\frac{{\rm d}p_a}{{\rm d}t} = -q_a[1 + \epsilon(p_a^2 + q_a^2)] - \gamma_a p_a + \alpha q_b + F\cos\Omega_1 t + S_1(p_A - p_a), \tag{18}$$

$$\frac{{\rm d}q_b}{{\rm d}t} = p_b[1 + \epsilon(p_b^2 + q_b^2)] - \gamma_b q_b + S_2(q_B - q_b), \tag{19}$$

$$\frac{{\rm d}p_b}{{\rm d}t} = -q_b[1 + \epsilon(p_b^2 + q_b^2)] - \gamma_b p_b + \alpha q_a + F\cos\Omega_2 t + S_2(p_B - p_b). \tag{20}$$

We study equations (13–20) numerically with the help of the fourth-order Runge-Kutta method with the integration step $\Delta t = 0.01$.

3 Two-time synchronism

Below, the system (13–20) is examined for selected values of the parameters. In the first example the Kerr nonlinearity is very small ($\epsilon = 10^{-9}$), the frequencies of the external fields are nearly equal $\Omega_1 \approx \Omega_2$, and all the damping constants are identical $\gamma_{a,A} = \gamma_{b,B}$. The second example deals with a Kerr nonlinearity $\epsilon = 10^{-1}$, the identical frequencies $\Omega_1 = \Omega_2$ and distinctly different damping constants $\gamma_{a,A} \ll \gamma_{b,B}$.

The condition of small Kerr coupling ϵ is met *e.g.* in modern optical fibers. The coupling Kerr constant is dependent here on the so-called normalized frequency of modes in a waveguide. We can change this parameter by choosing the appropriate optical frequency, material and geometrical properties of a fiber. Roughly speaking, choosing the normalized transverse wavenumbers of a field in a fiber we are able to change the coupling Kerr constants by changing the normalized frequency of modes. In certain types of fibers for small normalized frequencies we can obtain a very small Kerr constant [35].

3.1 Example 1. $S_1 \neq S_2$ and $\gamma_A = \gamma_B = \gamma_a = \gamma_b$

The system (13–20) starts from the initial conditions $\{q_A(0), p_A(0), q_B(0), p_B(0), q_a(0), p_a(0), q_b(0), p_b(0)\} = \{100, 0, 100, 0, 1, 0, 1, 0\}$ and the following fixed parameters $\gamma_{A,B} = \gamma_{a,b} = 0.001$, $\epsilon = 10^{-9}$, $\alpha = 0.04$, $F = 200$, $\Omega_1 = 1$ and $\Omega_2 = 1.05$.

Let us first briefly describe the dynamics of the master coupler governed by equations (13–16). For $t > 0$ due to different frequencies Ω_1 and Ω_2, the states of the oscillators **A** and **B** are always different *i.e.* $q_A(t) \neq q_B(t)$ and $p_A(t) \neq p_B(t)$. The autonomized spectrum of Lyapunov exponents for the system (13–16) computed by the method of Wolf *et al.* [37] is given by $\{0.008, 0.004, 0.000, -0.007, -0.010\}$, which means that the master coupler is hyperchaotic. It is interesting that for $\alpha = 0$ neither **A** nor **B** is chaotic, both oscillators behave quasiperiodically. The Lyapunov exponents of the slave coupler, which is a copy of the master coupler are identical.

Let us now concentrate on the master-slave dynamics. If the feedback terms in equations (17–20) are switched off, the slave coupler is independent of the master coupler. Mathematically, the set of equations (13–20) consists of two independent sets: (13–16) and (17–20) which physically correspond to the separate couplers. These separate hyperchaotic couplers generate irregular revivals and collapses (Fig. 2) whose pattern resembles the temporal structure of voice [25]. As time goes on, a trajectory, for example $q_a = q_a(t)$, with chaotically modulated amplitude passes through the equilibrium position $q_a = 0$ at regular intervals of $\sim (\Omega_1 + \Omega_2)^{-1}$. This regularity is similar to that which appears in beats generated by a linear system. However, in contradistinction to linear systems, a number of revivals (collapses) generated by a chaotic system and observed in a fixed interval cannot be determined as a function of the mismatch between the frequencies of the input fields. A beating frequency does not exists for beats with chaotic envelopes.

Let us now consider synchronization of the beats presented in Figure 2, when the feedback terms are switched on at the time $t_0 = 480$. The choice of the initial time $t_0 = 480$ is motivated by the fact that for this time the states of the master and slave couplers are distinctly different as clearly seen in Figure 2. The synchronization time T_s is defined as $T_s = t_s - t_0$, where t_s is defined as the time after which the quantity $q_{A,B} - q_{a,b}$ takes values lower than 10^{-3}. The dynamics of the synchronization is strongly different for the cases $S_1 \neq S_2$ and $S_1 = S_2$. For $S_1 = S_2$ the synchronization times for the pairs of oscillators $(\mathbf{a}, \mathbf{A})$ and $(\mathbf{b}, \mathbf{B})$ are the same. However, for the control parameter $S_1 \neq S_2$ we can observe two different times of synchronization $T_s^{(a,A)}$ and $T_s^{(b,B)}$ for the master-slave oscillators $(\mathbf{a}, \mathbf{A})$ and $(\mathbf{b}, \mathbf{B})$, respectively. This two-time synchronism is illustrated in Figure 3 for the values $S_1 = 5$ and $S_2 = 0.025$. The functions $\Delta_{(a,A)} = q_a - q_A$ and $\Delta_{(b,B)} = q_b - q_B$, being a measure of synchronization for the appropriate pairs of oscillators, show that the synchronization process for the pair $(\mathbf{a}, \mathbf{A})$ is faster ($T_s^{(a,A)} = 409$) than for the pair $(\mathbf{b}, \mathbf{B})$ for which $T_s^{(b,B)} = 790$. Identical results also hold for $p_a - p_A$ and $p_b - p_B$. A detailed numerical analysis shows that the difference $\Delta = T_s^{(b,B)} - T_s^{(a,A)}$ decreases exponentially to zero with increasing value of the interaction parameter α. Therefore, the strong linear interaction between the oscillators in the coupler leads, in practice, to disappearance of the two-time synchronism. The efficiency of the synchronization process depends on the values of α, S_1 and S_2. By way of example, this is illustrated in Figure 4, where the synchronization times $T_s^{(a,A)}$ and $T_s^{(b,B)}$ are presented as functions of the control parameter S_2 (for the fixed values of $\alpha = 0.04$ and $S_1 = 5$). As shown, the pair of oscillators $(\mathbf{a}, \mathbf{A})$ always synchronizes earlier then the pair $(\mathbf{b}, \mathbf{B})$, which is a consequence of the fact that the synchronization signal in the first channel is much stronger than that in the second channel ($S_1 > S_2$). If the value S_2 tends to S_1, then the difference between $T_s^{(a,A)}$ and $T_s^{(b,B)}$ vanishes and finally we observe only one-time synchronization *i.e.* $T_s^{(a,A)} = T_s^{(b,B)}$.

The two-time synchronization also occurs for $S_2 < 0.01$ (not shown in Fig. 4 as long synchronization times are not important in communication technique). If $S_2 \to 0$, the times $T_s^{(a,A)}$ and $T_s^{(b,B)}$ tend to infinity.

The question is what is the effect of the choice of t_0 on the results. The numerical analysis shows that the individual synchronization times $T_s^{(b,B)}$ and $T_s^{(a,A)}$ depend on the time t_0, that is, the time at which the feedback terms are switched on. Because of $S_1 \neq S_2$ we have $T_s^{(a,A)} \neq T_s^{(b,B)}$, which means that the pairs $(\mathbf{a}, \mathbf{A})$ and $(\mathbf{b}, \mathbf{B})$ have always different synchronization times. If $S_1 > S_2$ then the pair

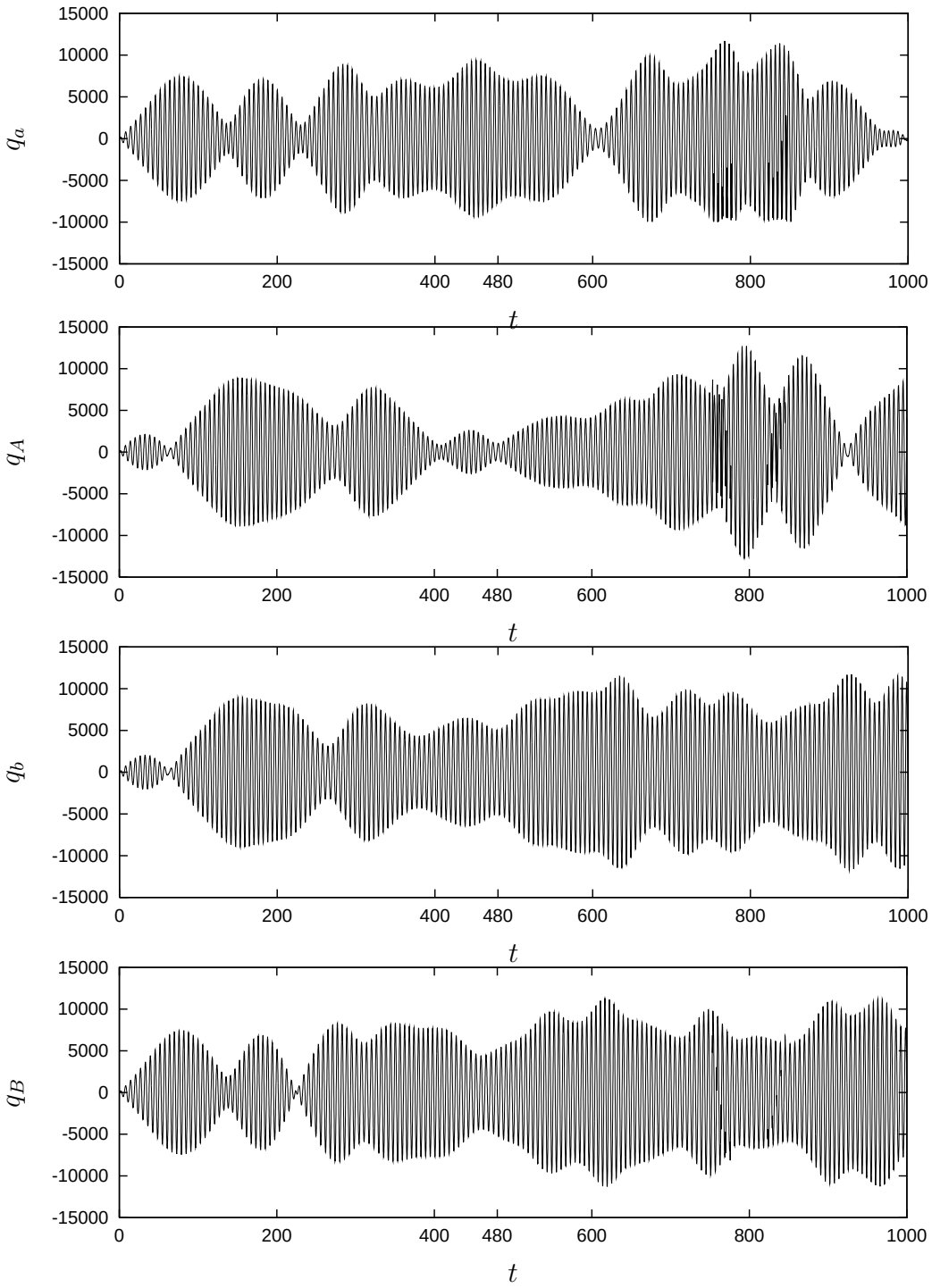

Fig. 2. Evolution of q_a, q_A, q_b and q_B *vs.* t for equations (13–20) if $S_1 = S_2 = 0$. The other parameters are: $\gamma_{A,B} = \gamma_{a,b} = 0.001$, $\epsilon = 10^{-9}$, $\alpha = 0.04$, $F = 200$, $\Omega_1 = 1$ and $\Omega_2 = 1.05$.

$(\mathbf{a}, \mathbf{A})$ synchronizes faster then the pair $(\mathbf{b}, \mathbf{B})$ or inversely if $S_2 > S_1$.

3.2 Example 2. $S_1 = S_2 = S$ and $\gamma_{a,A} \ll \gamma_{b,B}$

The two-time synchronism can appear in the system (13–20) not only if $S_1 \neq S_2$. This behavior is also observed for $S_1 = S_2 = S$, if instead of the identical damping constants, the couplers have different damping constants satisfying the relation $\gamma_{a,A} \ll \gamma_{b,B}$. Let us suppose that $\gamma_{a,A} = 0.05$ and $\gamma_{b,B} = 0.5$, which indicates that the second oscillators in both couplers are much stronger damped than the first ones. Here, the system (13–20) starts from the initial conditions $\{q_A(0), p_A(0), q_B(0), p_B(0),\ q_a(0), p_a(0), q_b(0), p_b(0)\}$=$\{1, 0, 3, 4, 1, -2, 3, 10\}$ and the following fixed parameters: $\epsilon = 0.1$, $\alpha = 0.4$, $F = 200$ and

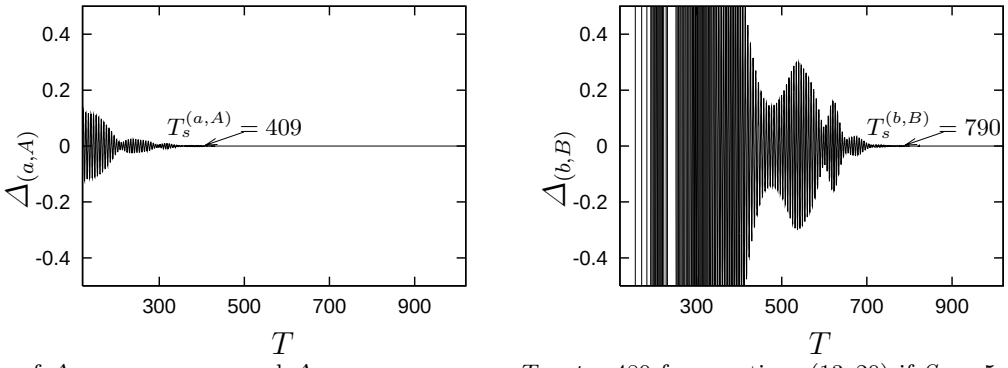

Fig. 3. Evolution of $\Delta_{(a,A)} = q_a - q_A$ and $\Delta_{(b,B)} = q_b - q_B$ *vs.* $T = t - 480$ for equations (13–20) if $S_1 = 5$ and $S_2 = 0.025$. The other parameters are: $\gamma_{A,B} = \gamma_{a,b} = 0.001$, $\epsilon = 10^{-9}$, $\alpha = 0.04$, $F = 200$, $\Omega_1 = 1$ and $\Omega_2 = 1.05$.

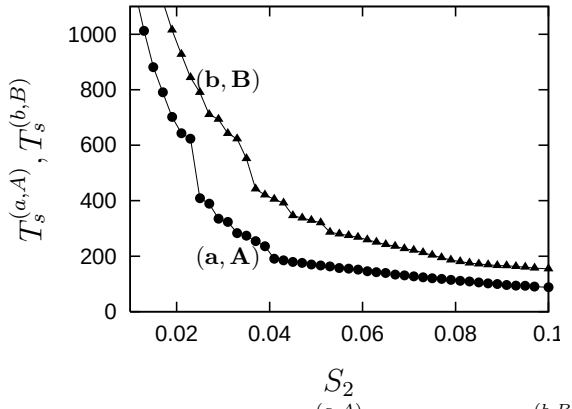

Fig. 4. Synchronization times $T_s^{(a,A)}$ (bullets) and $T_s^{(b,B)}$ (triangles) *vs.* S_2 for equations (13–20). The other parameters are: $\gamma_{A,B} = \gamma_{a,b} = 0.001$, $\epsilon = 10^{-9}$, $\alpha = 0.04$, $F = 200$, $\Omega_1 = 1$, $\Omega_2 = 1.05$ and $S_1 = 5$.

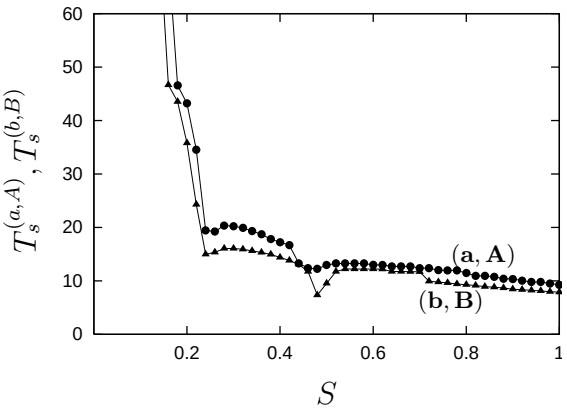

Fig. 5. Synchronization times $T_s^{(a,A)}$ (bullets) and $T_s^{(b,B)}$ (triangles) *vs.* S for the system (13–20), where $S = S_1 = S_2$. The other parameters are: $\gamma_{a,A} = 0.05$, $\gamma_{b,B} = 0.5$, $\epsilon = 10^{-1}$, $\alpha = 0.4$, $F = 200$ and $\Omega_{1,2} = 0.55$.

$\Omega_{1,2} = 0.55$. The dynamics of the system (13–20) is studied for the selected values of $S = S_1 = S_2$.

The dynamics of the master coupler differs from that described in Section 3.1. There are no beats here. For $\alpha = 0$ the oscillators **A** and **B** become independent subsystems. Then, the oscillator **A** manifests chaotic behavior forming a chaotic attractor in phase space, whereas the oscillator **B** is nonchaotic and tends to a limit cycle (see Fig. 1 in Ref. [32]). The autonomized Lyapunov spectra for **A** and **B** oscillators are $\{0.08, 0.00, -0.23\}$ and $\{0.00, -0.55, -0.90\}$, respectively. For individual values of $\alpha \neq 0$, the oscillators **A** and **B** interact with each other and can be chaotic or not [3,32], depending on the value of α. For $\alpha = 0.4$ they behave chaotically as clearly seen from the spectrum of Lyapunov exponents given by $\{0.06, 0.00, -0.21, -0.63, -0.80\}$. The Lyapunov coefficients of the slave coupler are identical to those of the master coupler.

Let us now consider the dynamics of synchronization for the system (13–20) putting $S_1 = S_2 = S$. The feedback terms are switched on at the time $t_0 = 100$ in order to eliminate the transient behavior. The synchronization time T_s is determined as $T_s = t_s - t_0$, where t_s is defined as the time after which the quantities $q_a - q_A$ and $q_b - q_B$ are lower than 10^{-3}. It is interesting to note that for $\gamma_{b,B} \gg \gamma_{a,A}$ the pair $(\mathbf{b}, \mathbf{B})$ synchronizes earlier than the pair $(\mathbf{a}, \mathbf{A})$. This situation takes place for any value of S. Consequently, we observe two different times of synchronization $T_s^{(a,A)}$ and $T_s^{(b,B)}$ satisfying the relation $T_s^{(a,A)} > T_s^{(b,B)}$ as illustrated in Figure 5. As seen the synchronization times $T_s^{(a,A)}$ and $T_s^{(b,B)}$ are small in comparison to those presented in Figure 4. In the range $0.4 < S < 0.5$ two sharp minima appear. The synchronization time $T_s^{(b,B)}$ is particularly small. If we change the time t_0 that is the time at which the feedback terms are switched on the presented anomalies vanish.

The behavior presented in Figure 5 suggests an additional question, namely, what is the effect of the damping constants different from those in Figure 5 on the function $|\Delta| = |T_s^{(b,B)} - T_s^{(a,A)}|$ describing the difference between the synchronization times. The calculations show, that the quantity $|\Delta|$ increases with increasing difference between the damping constants $\gamma_{a,A}$ and $\gamma_{b,B}$. If $\gamma_{a,A} > \gamma_{b,B}$ then the pair $(\mathbf{a}, \mathbf{A})$ synchronizes faster then the pair $(\mathbf{b}, \mathbf{B})$ and inversely if $\gamma_{b,B} > \gamma_{a,A}$.

4 Induced synchronization

The dynamics of synchronization examined in Sections 3.1 and 3.2 concerns a two-channel process. Let us now

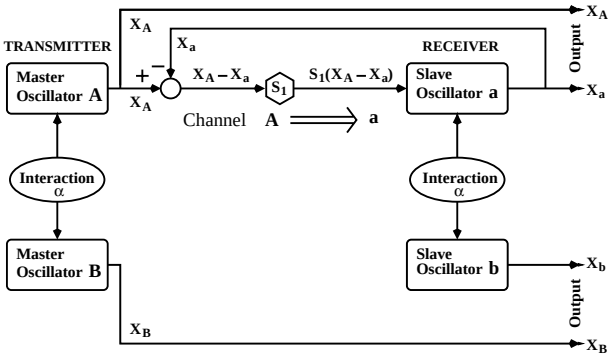

Fig. 6. One-channel synchronization. Is it possible to synchronize the pair $(\mathbf{b}, \mathbf{B})$ without a signal from **B** to **b**?

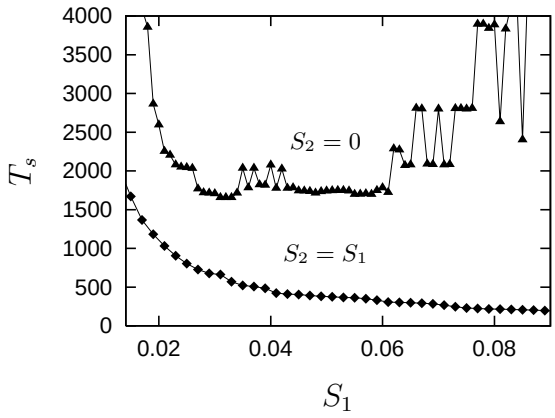

Fig. 7. A comparison between the synchronization times for one-channel ($S_1 \neq 0$, $S_2 = 0$; triangles) and two-channel ($S_2 = S_1$; diamonds) synchronization processes. Synchronization time T_s is plotted *vs.* S_1. The parameters of the system (13–20) are: $\gamma_{a,A} =$, $\gamma_{b,B} = 0.001$, $\epsilon = 10^{-9}$, $\alpha = 0.04$, $F = 200$, $\Omega_1 = 1$ and $\Omega_2 = 1.05$.

suppose that in the schematic diagram (Fig. 1) only the signal from the master subsystem **A** is transmitted to its slave counterpart **a**, whereas the second signal from **B** to **b** is turned off (see, Fig. 6). Below, we compare the two-channel dynamics of synchronization with its one-channel version.

4.1 Example 1. $S_1 \neq 0$, $S_2 = 0$ and $\gamma_A = \gamma_B = \gamma_a = \gamma_b$

We solve now equations (13–20) for $S_1 \neq 0$ and $S_2 = 0$. Below, we consider the synchronization times $T_s^{(a,A)}$ and $T_s^{(b,B)}$ as a function of S_1 for a fixed value $S_2 = 0$. The other parameters are as those in Section 3.1. The numerical analysis shows that for the one-channel synchronization process, $T_s^{(a,A)}$ and $T_s^{(b,B)}$ are approximately equal *i.e.* $T_s^{(a,A)} \approx T_s^{(b,B)} = T_s$. Therefore, in practice, the pairs $(\mathbf{a}, \mathbf{A})$ and $(\mathbf{b}, \mathbf{B})$ have the same synchronization time (denoted in Fig. 7 by triangles). This nearly one-time behavior in contradistinction to the distinct two-time behavior (triangles and bullets in Fig. 4) is caused by the small differences between the values $S_2 = 0$ and $0 < S_1 < 0.09$. For $S_2 = 0$ and $S_1 > 0.09$ synchronization does not occur. However, the main difference between Figures 4 and 7 is that the synchronization times for the two-channel process decrease exponentially with increasing values of the control parameter, whereas for its one-channel version the synchronization process has a local character. Namely, the fastest synchronization takes place at $S_1 = 0.032$ and then the synchronization time takes the minimum value $T_s = 1655$. It is interesting to note that in the range $0.041 < S_1 < 0.061$ the synchronization time reaches a nearly constant value. The average synchronization time in this region is equal to $\langle T_s \rangle \approx 1700$. As seen from Figure 7 (triangles), the one-channel synchronization process is the most effective in the range $0.025 < S_1 < 0.061$, that is when $S_1 \approx \alpha$. In the range $S_1 < 0.01$ and $S_1 > 0.1$ the synchronization is not observed.

It is also interesting to compare one-channel synchronization $(S_1 \neq 0, S_2 = 0)$ with its two-channel version satisfying the condition $S_1 = S_2$. In this case the synchronization times for the pairs $(\mathbf{a}, \mathbf{A})$ and $(\mathbf{b}, \mathbf{B})$ are

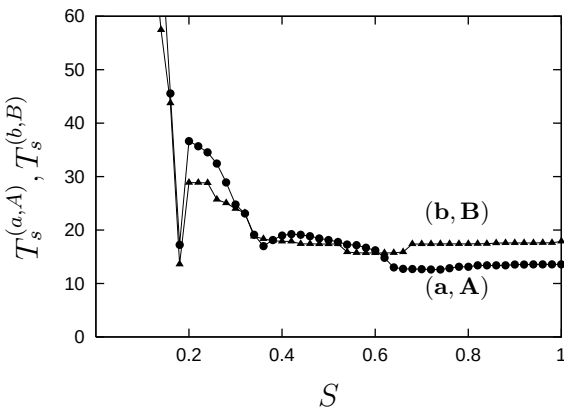

Fig. 8. Synchronization times $T_s^{(a,A)}$ (bullets) and $T_s^{(b,B)}$ (triangles) *vs.* S for the system (13–20), where $S_1 = S$, $S_2 = 0$. The other parameters are: $\gamma_{a,A} = 0.05$, $\gamma_{b,B} = 0.5$, $\epsilon = 10^{-1}$, $\alpha = 0.4$, $F = 200$ and $\Omega_{1,2} = 0.55$.

equal. The comparison is presented in Figure 7. The dynamics of the one-channel synchronization (triangles) differs strongly from its two-channel version (diamonds). For $S_2 = S_1$, the synchronization time T_s decreases nearly exponentially with increasing values of S_1, whereas for $S_1 \neq 0, S_2 = 0$ this relation does not hold. The efficiency of the induced synchronization $(S_1 \neq 0, S_2 = 0)$ is always lower than the synchronization forced by two channels and satisfying the relation $S_2 = S_1$.

4.2 Example 2. $S_1 \neq 0$, $S_2 = 0$ and $\gamma_{a,A} \ll \gamma_{b,B}$

Numerically, we study here the system (13–20) with $S_2 = 0$ and $S_1 = S$. The other parameters are the same as in Section 3.2. Here, two-time synchronism presented in Figure 8, similarly as in the two-channel process (Fig. 5), follows from by the condition $\gamma_{a,A} \ll \gamma_{b,B}$. However, there is one important difference between these figures. In the case presented in Figure 8, for $S > 0.62$ the first pair $(\mathbf{a}, \mathbf{A})$

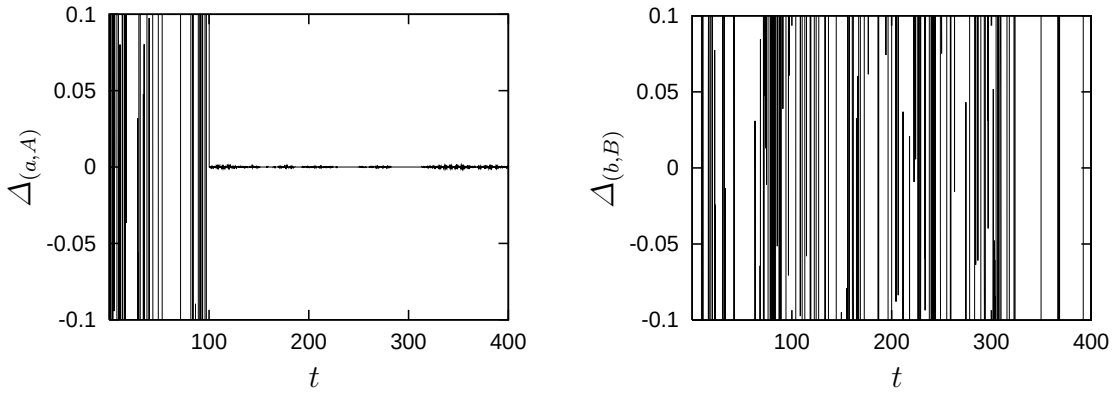

Fig. 9. Evolution of $\Delta_{(a,A)} = q_a - q_A$ and $\Delta_{(b,B)} = q_b - q_B$ *vs.* t for equations (13–20) if $S_1 = 60$ and $S_2 = 0$. The other parameters are: $\gamma_{A,B} = \gamma_{a,b} = 0.05$, $\epsilon = 10^{-1}$, $\alpha = 0.01$, $F = 200$ and $\Omega_{1,2} = 0.55$.

always synchronizes earlier than the second $(\mathbf{b}, \mathbf{B})$, whereas, for $S < 0.62$ we observe the same behavior (apart from a few points) as in Figure 5, *i.e.* the second pair synchronizes earlier then the first one. Let us emphasize that the second pair is synchronized, though the master subsystem **B** does not send a signal to the slave subsystem **b**.

It interesting that for $\gamma_{a,A} = 0.05$, $\gamma_{b,B} = 0.5$ and $\alpha = 0.4$, the synchronization of the system (13–20), with $S_1 = 0$ and $S_2 \neq 0$, which corresponds to the following simplified diagram

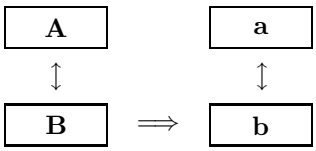

is not possible for any value of S_2. In other words, for the parameters considered, the change of the upper channel $\mathbf{A} \Rightarrow \mathbf{a}$ in the lower $\mathbf{B} \Rightarrow \mathbf{b}$ exclude any synchronization. Physically, the damping constant $\gamma_{b,B} = 0.5$ is too high in order to force synchronization of the two couplers through the lower channel.

4.3 Example 3. Partial synchronization

If $S_2 = 0$ and the interaction parameter α is very small in comparison to the value S_1 (but sufficient to generate strong chaos or hyperchaos in the coupler) then the induced synchronization can be partial. It means that the first pair $(\mathbf{a}, \mathbf{A})$ in Figure 6 is synchronized, whereas the second pair $(\mathbf{b}, \mathbf{B})$ is not. This effect is easy to get in the system (13–20) if $S_1 = 60$, $S_2 = 0$, $\gamma_{A,B} = \gamma_{a,b} = 0.05$ and $\alpha = 0.01$. The other parameters and the initial conditions are the same as in Section 3.2. The feedback term is turned on at the time $t_0 = 100$. For $\alpha = 0.01$ the coupler behaves hyperchaotically. The appropriate spectrum of Lyapunov exponents is $\{0.09, 0.08, 0.00, -0.22. - 0.23\}$. For $\alpha = 0$ both oscillators do not form a coupler. They are independent, identical and chaotic – the spectrum is $\{0.08, 0.00, -0.23\}$. As follows from Figure 9, synchronization of the first pair is nearly immediate after turning on a very strong feedback signal ($S_1 = 60$). On the other hand, the interaction between the oscillators within the coupler is so weak ($\alpha = 0.01$) that it is not able to force synchronization of the second pair $(\mathbf{b}, \mathbf{B})$. If $\alpha = 0$ the pair $(\mathbf{b}, \mathbf{B})$ is not synchronized *ex definitione* because $S_2 = 0$, and synchronization of the pair $(\mathbf{a}, \mathbf{A})$ can be achieved for a very small feedback signal, for example $S_1 = 0.1$ *i.e.* the feedback small in comparison to $S_1 = 60$ when the α-interaction is switched on.

5 Conclusions

Generally, the dynamics of the one-channel synchronization process is different from its two-channel version. In the one-channel process presented in Figure 6 the pair $(\mathbf{b}, \mathbf{B})$ is synchronized, though the master subsystem **B** does not send a signal to the slave subsystem **b**. Synchronization of the pair $(\mathbf{b}, \mathbf{B})$ is forced only by the first channel $\mathbf{A} \Rightarrow \mathbf{a}$, and the effect is termed induced synchronization. This effect, to our knowledge has been studied numerically in an optical system for the first time. Synchronization of the complex output signals $X_A = X_a$ and $X_B = X_b$ is equivalent in obvious way to intensity synchronization $X_A^* X_A = X_a^* X_a$ and $X_B^* X_B = X_b^* X_b$. The occurrence of two-time synchronism and the induced synchronization in the dynamical systems presented schematically in Figures 1 and 6 seems not unique and rather common. To observe these effects we can also use instead of two interacting Kerr oscillators, typical mechanical systems, for example; the Duffing models considered in [38, 39] or other two high-dimensional systems. However, the effect of induced synchronization becomes more and more difficult to achieve if the set-up presented in Figure 6 is supplemented by additional subsystems $\mathbf{C}, \mathbf{D}, ...$ and $\mathbf{c}, \mathbf{d}, ...$ In this way we build up a kind of a multilayer coupler. The induced synchronization effect and two-time synchronism are presented for the systems with different Kerr nonlinearities. The induced synchronization seems to have potential application in secure communication to hide messages [22]. The appropriate materials useful for the generation of different types of chaotic and hyperchaotic signals (for example, beats with chaotic envelopes) could be optical systems consisting of a pair of coupled Kerr fibers [35,40–43].

References

1. N. Platt, E.A. Spiegel, C. Tresser, Phys. Rev. Lett. **70**, 279 (1993)
2. Y.C. Lai, C. Grebogi, Phys. Rev. E **52**, R3313 (1995)
3. P. Szlachetka, K. Grygiel, *Modern Nonlinear Optics*, Part 2, Advances in Chemical Physics, edited by M.W. Evans (J. Wiley & Sons, 2001), Vol. 119, pp. 353-427
4. K. Grygiel, P. Szlachetka, Int. J. Bifurcat. Chaos **12**, 635 (2002)
5. S. Boccaletti, J. Kurths, G. Osipov, D.L. Valladares, C.S. Zhou, Phys. Rep. **366**, 1 (2002)
6. L.M. Pecora, T.L. Carroll, Phys. Rev. Lett. **64**, 821 (1990)
7. L.M. Pecora, T.L. Carroll, Phys. Rev. A **44**, 2374 (1991)
8. J.F. Heagy, T.L. Carroll, L.M. Pecora, Phys. Rev. E **50**, 1874 (1994)
9. L.M. Pecora, T.L. Carroll, G.A. Johnson, D.J. Mar, J.F. Heagy, Chaos **7**, 520 (1997)
10. K. Pyragas, Phys. Rev. E **54**, R4508 (1996)
11. Y. Zhang, G. Hu, H.A. Cerdeira, S. Chen, T. Braun, Y. Yao, Phys. Rev. E **63**, 026211-1 (2001)
12. N.F. Rulkov, M.M. Sushchik, L.S. Tsimring, H.D.I. Abarbanel, Phys. Rev. E **51**, 980 (1995)
13. L.M. Pecora, T.M. Carroll, D.F. Heagy, Phys. Rev. E **52**, 3420 (1995)
14. L. Kocarev, U. Parlitz, Phys. Rev. Lett. **76**, 1816 (1996)
15. N.F. Rulkov, C.T. Lewis, Phys. Rev. E **63**, 065204(R) (2001)
16. A.S. Pikovsky, M.G. Rosenblum, G.V. Osipov, J. Kurtz, Physica D **104**, 219 (1997)
17. M.G. Rosenblum, A.S. Pikovsky, J. Kutrz, Phys. Rev. Lett. **76**, 1804 (1996)
18. K. Cuomo, A.V. Oppenheim, Phys. Rev. Lett. **71**, 65 (1993)
19. L. Kocarev, U. Parlitz, Phys. Rev. Lett. **74**, 5028 (1995)
20. S. Boccaletti, A. Farini, F.T. Arecchi, Phys. Rev. E **55**, 4979 (1997)
21. M. Hasler, Int. J. Bifurcat. Chaos **8**, 647 (1998)
22. S. Boccatetti, C. Grebogi, Y.-C. Lai, H. Mancini, D. Maza, Phys. Rep. **329**, 103 (2000)
23. Teh-Lu Liao, Shin-Hwa Tsai, Chaos Solitons & Fractals **11**, 1387 (2000)
24. J.H. Peng, E.J. Ding, M. Ding, W. Yang, Phys. Rev. Lett. **76**, 904 (1996)
25. K.M. Short, A.T. Parker, Phys. Rev. E **58**, 1159 (1998)
26. M.K. Ali, J. Fang, Phys. Rev. E **55**, 5285 (1997)
27. H.G.L. Rahman, Phys. Rev. Lett. **65**, 1575 (1990)
28. R. Roy, K.S. Thornburg Jr, Phys. Rev. Lett. **72**, 2009 (1994)
29. A. Hohl, A. Gavrielides, T. Erneux, V. Kovanis, Phys. Rev. Lett. **78**, 4745 (1997)
30. P. Colet, R. Roy, Opt. Lett. **19**, 2056 (1994)
31. G.D. van Wiggeren, R. Roy, Int. J. Bif. Chaos **9**, 2129 (1999)
32. K. Grygiel, P. Szlachetka, J. Opt. B: Quant. Semiclass. Opt. **3**, 104 (2001)
33. K. Grygiel, Opt. Commun. **204**, 391 (2002)
34. J. Peřina Jr, J. Peřina, *Quantum Statistics of Nonlinear Optical Couplers* in *Progress in Optics*, edited by E. Wolf (Elsevier Science, 2000), Vol. 41, pp. 361-419
35. K. Okamoto, *Fundamentals of Optical Waveguides* (Academic Press, 2000)
36. K. Pyragas, Phys. Lett. A **170**, 421 (1992)
37. A. Wolf, J.B. Swift, H.L. Swinney, J.A. Vastano, Physica D **16**, 285 (1985)
38. S.P. Raj, S. Rajasekar, K. Murali, Phys. Lett. A **264**, 283 (1999)
39. J. Kozlowski, U. Parlitz, W. Lauterborn, Phys. Rev. **51**, 1861 (1995)
40. K. Grygiel, P. Szlachetka, Opt. Commun. **177**, 425 (2000)
41. S.M. Jensen, IEEE J. Quant. Electron. **QE-18**, 1580 (1982)
42. V.M. Kenkre, D.K. Campbell, Phys. Rev. B **34**, 4959 (1996)
43. A. Chefles, S.M. Barnet, J. Mod. Opt. **43**, 709 (1996)